SCIENTIFIC REP⚙RTS

OPEN

Geometry, Electronic Structure, and Pseudo Jahn-Teller Effect in Tetrasilacyclobutadiene Analogues

Yang Liu[1], Ya Wang[1] & Isaac B. Bersuker[2]

We revealed the origin of the structural features of a series of tetrasilacyclobutadiene analogues based on a detailed study of their electronic structure and the pseudo Jahn-Teller effect (PJTE). Starting with the D_{4h} symmetry of the Si_4R_4 system with a square four-membered silicon ring as a reference geometry, and employing ab initio calculations of energy profiles along lower-symmetry nuclear displacements in the ground and several excited states, we show that the ground-state boat-like and chair-like equilibrium configurations are produced by the PJT interaction with appropriate excited sates. For Si_4F_4 a full two-mode $b_{1g}-b_{2g}$ adiabatic potential energy surface is calculated showing explicitly the way of transformation from the unstable D_{4h} geometry to the two equilibrium C_{2h} configurations via the D_{2h} saddle point. The PJTE origin of these structural features is confirmed also by estimates of the vibronic coupling parameters. For Si_4R_4 with large substituents the origin of their structure is revealed by analyzing the PJT interaction between the frontier molecular orbitals. The preferred chair-like structures of Si_4R_4 analogues with amido substituents, and heavier germanium-containing systems Ge_4R_4 (potential precursors for semiconducting materials) are predicted.

Cyclobutadiene and its derivatives have attracted extensive attention of researchers for many years[1–9]. Among all kinds of its derivatives tetrasilacyclobutadiene analogues (denoted as Si_4R_4 hereafter) are the hottest topics due to the rich silicon chemistry and expected novel applications as semiconducting materials[1,5,10]. Recently, the interest in these compounds was enhanced by the synthesis of $Si_4(EMind)_4$ (EMind $=1,1,7,7$-tetraethyl-3,3,5,5-tetramethyl-s-hydrindacen-4-yl), and its structural characterization with a distinctive planar-rhombic four-member silicon ring[11,12] (Fig. 1). Consequently, some new tetrasilacyclobutadiene or tetragermacyclobutadiene analogues that contain a planar-rhombic or puckered Si_4 ring[13,14], a slightly folded Ge_4 ring[15], or a puckered Si_3Ge ring with ylide structure[16] were synthesized. As the simplest member of Si_4R_4 family, the parent Si_4H_4 was predicted theoretically to have a puckered Si_4 ring with D_{2d} symmetry[2,5]. From the simplest Si_4H_4 to the complicated $Si_4(EMind)_4$ compound the central silicon skeleton undergoes several low-symmetry configuration changes of the reference square-planar geometry.

The origin of this variety of the molecular geometries in the Si_4R_4 and Ge_4R_4 series can be rationalized by employing the vibronic coupling theory in the form of the pseudo Jahn-Teller effect (PJTE)[17,18]. This statement follows from a more general conclusion that the Jahn-Teller effect for degenerate electronic states and the PJTE for both degenerate and nondegenerate (pseudodegenerate) states are the only source of spontaneous symmetry breaking in molecular systems and solids (see references in refs 17–19). In our case of nondegenerate electronic states the PJTE provides a reasonable picture of the structure and properties of the compounds under consideration. The method has been successfully applied to more simple carbon and silicon four-membered ring systems, such as C_4H_4[20], C_4F_4[7], Si_4[21], $Si_4H_4^{2+}$[22], as well as to a variety of other molecular systems (see[18,23–30] and references therein).

In this paper we report the results of a detailed analysis of the origin of the structural features of a series tetrasilacyclobutadiene analogues, Si_4R_4, including relatively large substituents R, as well as some other related systems, including Ge_4R_4, based on their electronic structure and vibronic coupling. Applying the PJTE theory, we reveal the lowest excited states that cause the distortion (puckering) of the high-symmetry planar configuration and estimate the vibronic coupling constants that control these distortions. This information provides also some clues for manipulation of the structure by means of external perturbations or substitutions, similar to the recently

[1]Academy of Fundamental and Interdisciplinary Sciences, Harbin Institute of Technology, Harbin, 150080, People's Republic of China. [2]Institute for Theoretical Chemistry, University of Texas at Austin, Austin, TX 78712, USA. Correspondence and requests for materials should be addressed to Y.L. (email: yang.liu@hit.edu.cn)
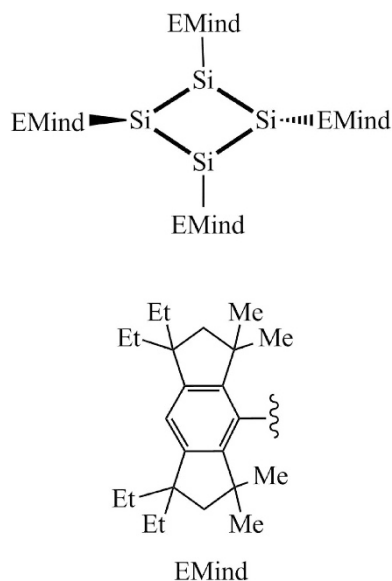
1

Figure 1. The 2-D structure of Si4(Emind)4 reported by Suzuki *et al.*[11].
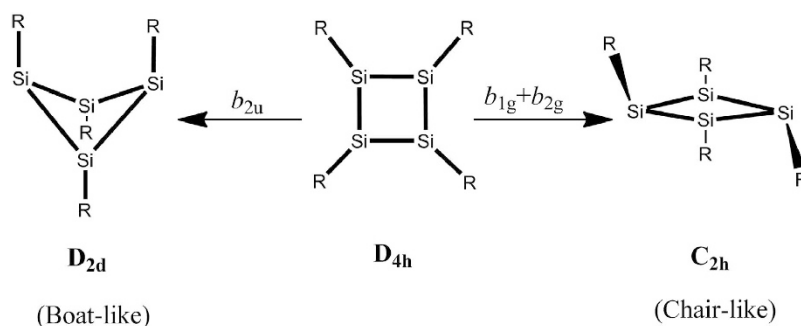

Figure 2. Two types of distortions of the highest-symmetry D_{4h} configuration of Si_4R_4 compounds induced by the PJTE: boat-like with D_{2d} and chair-like with C_{2h} symmetry.

suggested methods of restoring planarity in puckered hexa- and tetra-heterocyclic systems[31–33], thus inspiring the search of new materials with desired properties, in particular, other kinds of stable tetrasilacyclobutadiene analogues. Our theoretical prediction of stable structures of Si_4R_4 analogues with different substituents and Ge_4R_4 with bulky substituents is expected to provide also information for synthesizing new silicon or germanium four-member ring compounds and exploring their potential applications as semiconducting materials.

Results and Discussion

PJTE in the origin of Si_4R_4 geometries.
There are two typical equilibrium structures of Si_4R_4 analogues, the one with a puckered Si_4 ring as in Si_4H_4, which hereafter is denoted as a "boat-like" structure, and the other one with a planar-rhombic Si_4 ring and alternating pyramidal and planar bonded substituents at the silicon atoms, which is denoted as "chair-like" structure hereafter (Fig. 2). To rationalize the origin of these boat-like and chair-like structures of Si_4R_4 analogues we start with one of the simpler representatives, the Si_4F_4 molecule; it allows revealing the main mechanisms of formation of boat-like and chair-like structures that are similar for all the Si_4R_4 systems.

According to the general procedure, the PJTE formulation in this case starts from the highest symmetry D_{4h} configuration at which the molecule is square-planar with the central Si_4 ring forming a square and the four ligands symmetrically bonded. Its transformations to the lower symmetry configurations is realized by symmetrized b_{2u} type displacements toward the boat-like geometry and via combined $b_{1g} + b_{2g}$ displacements toward the chair-like configuration (Fig. 2). [Hereafter we employ small letters to denote the symmetry representations of both vibrational modes and molecular orbitals, and capital letters for electronic states]. Since the ground state in D_{4h} geometry is nondegenerate, according to the general theorem[17,18] the instabilities are induced by the pseudo Jahn-Teller (PJT) coupling to appropriate excited electronic states. To reveal the latter we calculate and analyze the energy profiles (the cross section of the adiabatic potential energy surface (APES)) of the electronic ground and low-lying excited states along these normal displacements. The results are shown in Fig. 3.

Consider first the instability along the b_{2u} coordinate Q_{b2u} of molecular puckering that leads to the boat-like structure with D_{2d} symmetry. Note that Q denotes normal coordinates, not atomic displacements. As seen from Fig. 3(a), along b_{2u} the D_{4h} configuration in the singlet ground state $1\,^1B_{2g}$ is unstable and distorts spontaneously up to the minimum point at $Q = 0.7$ Å which is the boat-like structure of Si_4F_4 of Fig. 2 (the role of the triplet state is outlined below). According to the group theory rules the lowest excited states that couple with $1\,^1B_{2g}$ via the b_{2u} mode in the D_{4h} symmetry are the $1\,^1A_{1u}$ and $2\,^1A_{1u}$ states, realizing the $(1\,^1B_{2g} + 1\,^1A_{1u} + 2\,^1A_{1u}) \otimes b_{2u}$ PJTE problem (the role of higher excited states is discussed in next section). Hence the formation of the boat-like structure in this system is due to the vibronic coupling with the excited $^1A_{1u}$ states. From the estimated vibronic coupling constants below it follows that the main contribution comes from the $1\,^1A_{1u}$ state. By comparing the electronic structures we can see that the $1\,^1B_{2g}$ state comes from the e_g^2 electronic configuration, while the $1\,^1A_{1u}$ state emerges from the electronic excitations of an e_g electron to the empty e_u orbital. The latter thus play an important role in the formation of boat-like structures.

The analysis of possible distortions along b_{1g} and b_{2g} is more complicated. From Fig. 3(b) we see that there is a hidden PJTE (meaning a sufficiently strong PJT interaction between two or more excited states that produces an additional global minimum with a distorted configuration, see ref. 29 for details): the PJT mixing of the three close excited states, $(1\,^1A_{1g} + 1\,^1B_{1g} + 2\,^1A_{1g}) \otimes b_{1g}$, produces an additional potential minimum at $Q_{b1g} = 1.1$ Å in which the Si_4 framework is rhombically distorted. On the other hand, the ground state ^1A_g is unstable with respect to the b_{2g} puckering, and it is a priori unclear where the global minimum might occur. This prompted further calculations of the two-dimensional part of the APES along two coordinates b_{1g} and b_{2g}. The results are illustrated in Fig. 4. We see that, indeed, the minimum in the energy profile along b_{1g} is just a saddle point, from which the system descends along b_{2g} to the global minima of C_{2h} symmetry with a chair-like structure of Fig. 2. The normal coordinates (Q_{b1g}, Q_{b2g}) of these two minima (read off the D_{4h} point) in Å are about $(0.74, \pm 0.62)$. To reveal the excited states involved in these PJTE distortions we calculated the energy profiles of the system along b_{2g} (shown in Fig. 3(c)) beginning from the point $Q_{b1g} = 0.74$ Å of Fig. 3(b).

The results shown in Fig. 4 together with the energy profiles in Fig. 3 illustrate the full picture of instabilities and distorted equilibrium-geometry formation of the Si_4F_4 molecule. In the highest symmetry configuration D_{4h} the system is unstable along b_{1g} (rhombic distortion of the Si_4 ring) due to the hidden PJTE problem $(1\,^1A_{1g} + 1\,^1B_{1g} + 2\,^1A_{1g}) \otimes b_{1g}$ mixing two excited electronic states, followed by the puckering distortion b_{2g} (emerging from the $(1\,^1A_g + 1\,^1B_{2g} + 1\,^1A_g) \otimes b_{2g}$ problem), resulting in an equilibrium chair-like structure at the minima of the APES (Fig. 2). On the other hand, as shown above, the APES of this system has another minimum along the b_{2u} displacements producing the boat-like equilibrium structure. However, because the two excited states $1\,^1A_{1g}$ and $1\,^1B_{1g}$ in the D_{4h} geometry are relatively very close, the hidden PJTE of their mixing along b_{1g} is much stronger than that of the $(1\,^1B_{2g} + 1\,^1A_{1u} + 2\,^1A_{1u}) \otimes b_{2u}$ problem, so the chair-like structure is lower in energy by 0.39 eV than the boat-like structure. The fully optimized chair-like and boat-like Si_4F_4 geometrical coordinates are given in the Supplementary data S1. By examining the $1\,^1B_{1g}$ excited state in the ab initio calculations we can see that dominant electronic configurations are produced by the electronic transitions from the occupied e_g to b_{1g} or a_{1g} empty molecular orbitals. The significant role of b_{1g} orbital in these interactions is discussed below in more detail.

Note that the triplet $^3A_{2g}$ ground state in the D_{4h} geometry is not significant with respect to observable structural features of Si_4F_4 because it is stable with respect to b_{1g} distortions that lead to the global minima with a singlet electronic state (Fig. 3(b)), at which point $^3A_{2g}$ is an excited state; its instability in D_{4h} along the b_{2u} mode leads to approximately the same boat-like minimum as in the singlet $1\,^1B_{2g}$ state (Fig. 3(a)) which, as shown above, is much higher in energy than the chair-like minimum.

Numerical estimation of the PJTE coupling parameters.

The qualitative picture, which reveals the excited electronic states producing the instability of the ground state, obtained in the previous section, can be enhanced quantitatively by estimates of the numerical values of the vibronic coupling parameters in the PJTE. First of all such numerical estimates are important to limit the number of excited states that produce significant contribution to the instability in a given direction. Indeed, in any polyatomic system the number of excited states is practically infinite, and for any given low-symmetry displacement Q there are always some excited states of relevant symmetry that contribute to the destabilization of the ground state. In general, this contribution is rather small, just lowering the curvature of the ground state from K_0 to $K_0 - p$, $p > 0$, and not producing instability, meaning $K_0 - p > 0$, (according to the general theory[17] the primary force constant without the vibronic coupling, $K_0 > 0$), and only low-lying excited states with sufficiently large contribution to the PJT destabilization of the ground state may be the reason of instability, and only in certain directions Q.

Assuming that there is only one such excited state producing instability in the Q direction, we come to the two-level PJTE problem. The primary force constants in the ground and the active excited state is denoted by K_1 and K_2, respectively, and the second order perturbation corrections to them from all the higher excited states of appropriate symmetry is defined by p_1 and p_2 in the PJTE energy matrix elements $W_{\Gamma\Gamma}$ and $W_{\Gamma'\Gamma'}$[23]:

$$W_{\Gamma\Gamma} = -2\sum_n \frac{|F_{\Gamma n}|^2}{E_n - E_\Gamma} Q^2 = -p_1 Q^2 \tag{1}$$

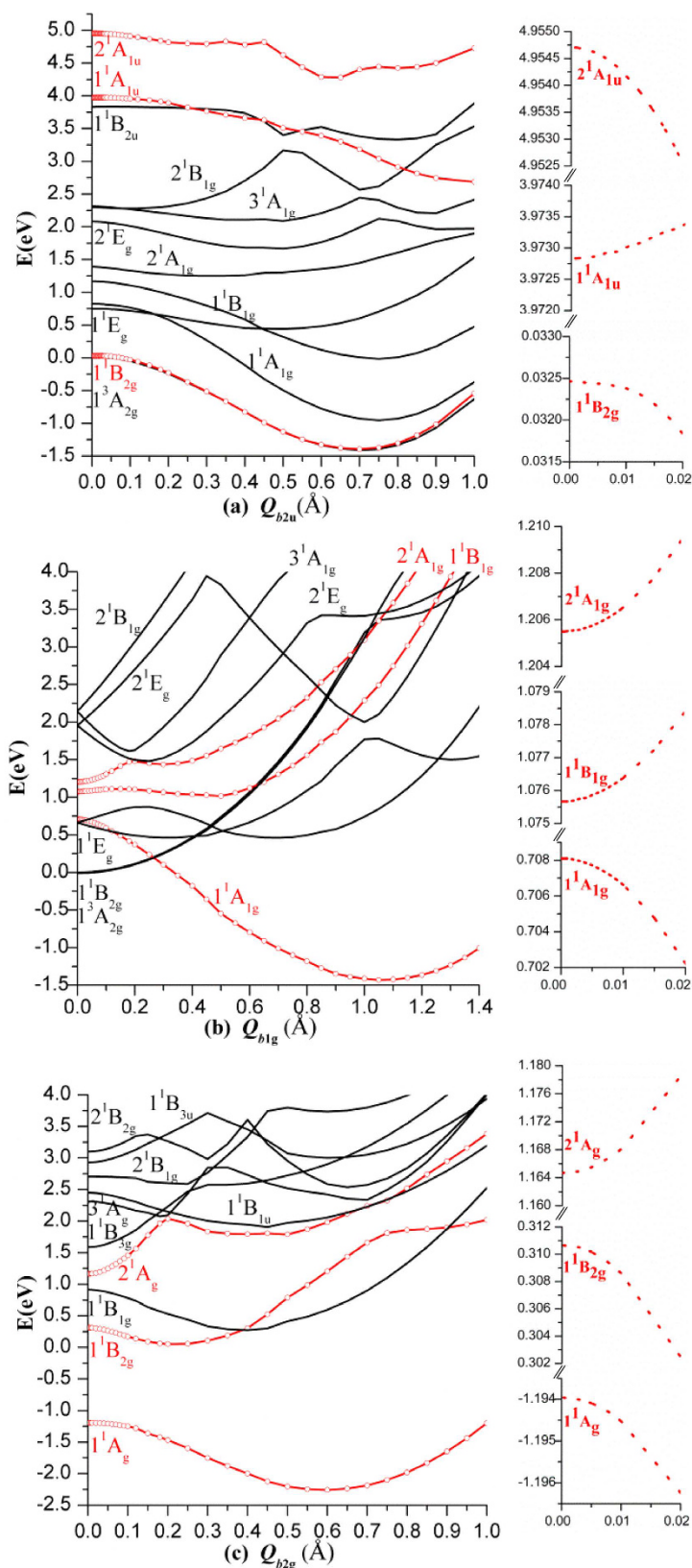$$W_{\Gamma'\Gamma'} = -2\sum_n \frac{|F_{\Gamma' n}|^2}{E_n - E_{\Gamma'}} Q^2 = -p_2 Q^2 \tag{2}$$

Figure 3. The potential energy profiles of the ground and low-lying excited states of the Si_4F_4 molecule along b_{2u} (**a**), b_{1g} (**b**) and b_{2g} (**c**) distortions by taking the energy of the D_{4h} configuration as the zero point. The lines in red with dots represent the coupling states, shown also in the inserts at small displacements (some states between $^1A_{1u}$ and 2^1A_{1u} in Fig. 3(a) are not shown, see Supplementary Fig. S2). The distortions along b_{2g} in Fig. 3(c) are conveniently started at $Q_{b1g} = 0.74$Å of Fig. 3(b), from which point there is a direct pass to the global minima shown in Fig. 4.
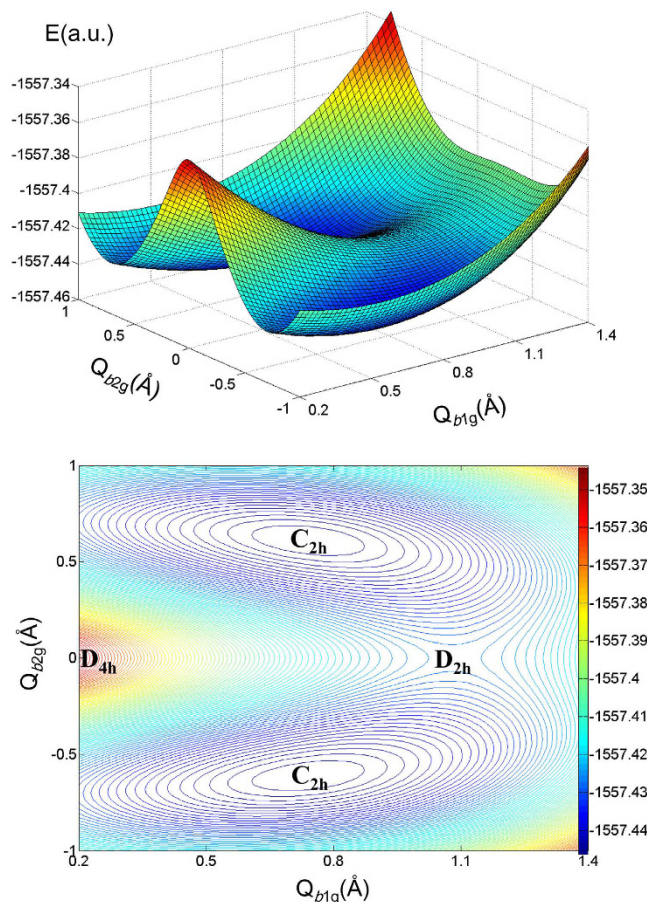
Figure 4. Calculated two-dimensional segment of the APES of the Si$_4$F$_4$ molecule (top) and its contour map (bottom) in the rhombic b_{1g} and puckering b_{2g} distortion coordinates.

Then, the APES $\varepsilon(Q)$ can be obtained from the secular equation of the perturbation theory:

$$\begin{vmatrix} \frac{1}{2}(K_1 - p_1)Q^2 - \varepsilon & FQ \\ FQ & \frac{1}{2}(K_2 - p_2)Q^2 + \Delta - \varepsilon \end{vmatrix} = 0 \tag{3}$$

where K_1, K_2, p_1 and p_2 are the primary force constants as explained above, F is the PJT vibronic coupling constant between the two states, and Δ is the energy gap of the two coupled states.

The roots of this secular equation are:

$$\varepsilon_{gr,ex} = \frac{1}{4}(K_1 - p_1 + K_2 - p_2)Q^2 + \frac{\Delta}{2} \mp \frac{\Delta}{2}$$
$$\times \sqrt{1 + \frac{1}{4\Delta^2}(K_1 - p_1 - (K_2 - p_2))^2\, Q^4 - \frac{1}{\Delta}\left((K_1 - p_1 - (K_2 - p_2)) - \frac{4F^2}{\Delta}\right)Q^2} \tag{4}$$

At small values of Q we get for the ground state:

$$\varepsilon_{gr} \approx \frac{1}{2}\left(K_1 - p_1 - \frac{2F^2}{\Delta}\right)Q^2 \tag{5}$$

Then the condition of instability at $Q = 0$ of the ground state due to the PJT vibronic coupling is:

$$K_1 - p_1 < \frac{2F^2}{\Delta} \tag{6}$$

We thus separated all the excited states that destabilize the ground state via the PJTE in two parts: (1) all the higher states with small contributions taken into account by means of a second order perturbation correction p to the curvature K_0, and (2) the lowest active excited state acting directly via the secular equation lowering the

Mode	$K_1 - p_1$ (eV/Å²)	$K_2 - p_2$ (eV/Å²)	$K_3 - p_3$ (eV/Å²)	F (eV/Å)	G (eV/Å)	Δ_1 (eV)	Δ_2 (eV)
b_{2u}	2.51	−0.42		2.87		3.94	
b_{1g}	0.27	0.43	−0.67	0.33	0.23	0.37	0.50
b_{2g}	4.07	−13.98	19.29	3.83	3.74	1.50	2.36

Table 1. The estimated parameters of the PJTE in Si₄F₄: primary force constants, linear vibronic coupling constants, and energy gaps to active excited states along b_{2u}, b_{1g} and b_{2g} distortions.

curvature by $\frac{2F^2}{\Delta}$. This means that if the chosen excited state is indeed the one responsible for the instability the numerical estimates should yield $K_1 - p_1 > 0$ and $K_1 - p_1 - \frac{2F^2}{\Delta} < 0$.

The direct *ab initio* calculation of these constants encounters difficulties (their calculation for some systems see in ref. 23). In the present paper we estimated them by fitting the solutions of the secular equation (4) to the *ab initio* data for the energy profiles of the corresponding states. For the b_{2u} distortion the PJTE two-level problem $(1^1B_{2g} + 1^1A_{1u}) \otimes b_{2u}$ yields satisfactory results listed in Table 1. The numerical value of $K_1 - p_1 - \frac{2F^2}{\Delta}$ is −1.67, which satisfies the condition of instability (6); the contribution of all the other active excited states is included in the second-order perturbation correction p_1. We checked the influence of the nearest one 2^1A_{1u}: its inclusion into the secular equation (7) below yields a very small contribution to the instability, thus justifying the two-level PJTE formulation for this case.

However, for the b_{1g} and b_{2g} instabilities only one active excited state does not yield positive $K_1 - p_1$ values, meaning higher excited electronic states should be included in the secular equation of direct PJT interaction. For a three-level problem the secular equation is:

$$
\begin{vmatrix}
\frac{1}{2}(K_1 - p_1)Q^2 - E & FQ & 0 \\
FQ & \frac{1}{2}(K_2 - p_2)Q^2 + \Delta_1 - E & GQ \\
0 & GQ & \frac{1}{2}(K_3 - p_3)Q^2 + \Delta_2 - E
\end{vmatrix} = 0
\tag{7}
$$

where in addition to the above denotations K_3 is the primary force constant for the third term, p_3 is the second order perturbation correction and G is the additional vibronic coupling constant to this term. Accordingly, the PJTE producing these distortions are $(1^1A_{1g} + 1^1B_{1g} + 2^1A_{1g}) \otimes b_{1g}$ and $(1^1A_g + 1^1B_{2g} + 2^1A_g) \otimes b_{2g}$, and the excited electronic states controlling these instabilities are 1^1B_{1g} and 2^1A_{1g} for the b_{1g} rhombic distortions, and 1^1B_{2g} and 2^1A_g for further b_{2g} puckering displacements in the rhombic configuration. The estimated PJTE constants are given in Table 1. The numerical results were evaluated by a fitting procedure with very small standard deviations of the residuals and the Pearson's correlation coefficients equal to 1. The negative values of $K–p$ in the excited states show that they are strongly influenced by the PJT coupling with higher electronic states.

Extension to Si₄R₄ compounds with bulky substituents. The description of the origin of the structural features of Si₄F₄ as due to the PJTE may serve as a prototype for the investigation of Si₄R₄ analogues with more complicated substituents, such as the mentioned above Si₄(EMind)₄. However, the larger size systems possess many close-in-energy electronic states and normal modes (due to much lower molecular symmetry than D₄ₕ) which make a full analysis of the structural features in terms of symmetry adapted electronic states for the system as a whole much more difficult. In this case (as in many similar chemical problems) a more simple description can be achieved by considering the PJTE in terms of frontier molecular orbitals (MO) (obtained from the electronic structure calculations) which may happen to be localized in a much reduced "active center", as in the case under consideration.

Figure 5 shows the highest occupied MO (HOMO), the next lower occupied MO (HOMO-1), and lowest unoccupied MO (LUMO) in the chair-like minima configurations of a series of Si₄R₄ with R as fluorine, phenyl, tetramethyl-phenyl, s-indacene, and EMind groups. We see that the electronic distributions of these frontier molecular orbitals are located mostly around the Si₄ ring which is thus the active center of the whole molecule. In other words, the bulky substituents reduce the formal molecular point group, but play a minor role in the key electronic and vibronic properties of active center of Si₄R₄ that control their geometry via the PJTE. Therefore we can use the PJTE formulations and results obtained for Si₄F₄ with the D₄ₕ high-symmetry configuration as a reference in exploring Si₄R₄ systems with bulky substituents. In the HOMO the electronic cloud is mainly on the σ bonding orbitals between two silicon atoms (to form the short diagonal), and non-bonding orbitals from the other two pyramidal silicon atoms (at the virtual long diagonal), with less charged density at the neighbor F or C atoms, and this HOMO electronic distribution is almost the same for all the Si₄R₄ systems.

Based on the same Si₄ ring active center and the same HOMO electronic distributions of the Si₄R₄ derivatives, we come to the prediction that they have the same kind of PJTE origin. By tracing this orbital distribution in the lowest ^1A_g singlet electronic state along b_{1g} and b_{2g} distortions in Si₄F₄ (Fig. 6) we found that the HOMO actually originates from the empty b_{1g} MO of the undistorted D₄ₕ configuration; it becomes a_g after distortion. As follows from the numerical data of the ab initio calculations illustrated in Fig. 6(a), the electronic distribution in this b_{1g} MO is mainly on the four σ^*_{Si-Si} anti-bonding orbitals; under the b_{1g} distortion it gradually becomes bonding σ_{Si-Si} for two diagonal silicon atoms, and non-bonding MO for the other two silicon atoms. Then along the
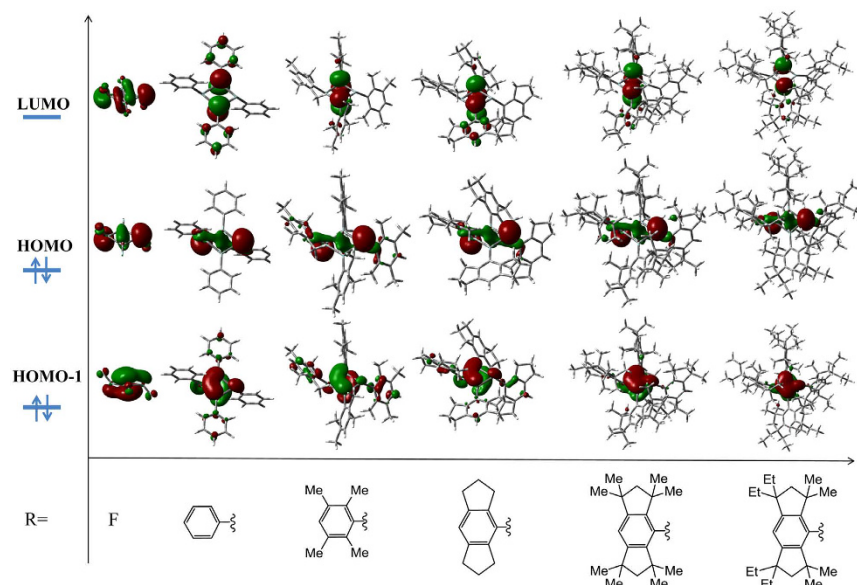
Figure 5. Calculated HOMO-1, HOMO, and LUMO of a series of trtrasilacyclobutadiene analogues Si_4R_4.
The charge distributions are located at mostly the central fragment Si_4 and the HOMO is essentially the same for all these compounds.

puckered b_{2g} mode the coplanar non-bonding MO of the latter turns to be located at the pyramidal positions, as shown in Fig. 6(b). In combination with the two-step distortions outlined above, we conclude that the initial b_{1g} MO in the undistorted high-symmetry configuration turns into the HOMO of Si_4F_4 in the chair-like structure. The changes in these charge distributions by distortions result from the admixture of excited states, and they take place spontaneously because this PJTE admixture of electronic states improves the bonding conditions and lowers the energy of the system by means of added covalency[17,18]. As expected and confirmed, the chair-like structures of Si_4R_4 compounds with bulky substituents R, including $Si_4(EMind)_4$, are qualitatively of the same PJTE origin as in the Si_4F_4 molecule.

Structural correlations in Si_4R_4 compounds controlled by the PJTE.

There are significant similarities and differences in the structural features of Si_4R_4 compounds with different R substituents. It follows from electronic structure calculations with geometry optimization[5] that Si_4H_4 has only one equilibrium boat-like geometry, while Si_4F_4, as well as Si_4Cl_4 and $Si_4(OH)_4$ have both boat-like and chair-like minima, and the chair-like minimum is lower in energy. Since all these low-symmetry structures are controlled by the PJTE, their similarities and differences can be rationalized by employing the PJTE theory. We demonstrate this statement by comparisons among the mentioned four Si_4R_4 systems, Si_4H_4, Si_4F_4, Si_4Cl_4 and $Si_4(OH)_4$.

In the simplest two-level presentation of the PJTE (see Eqs. (3–6)) the vibronic coupling of the electronic ground state of the system in the high-symmetry configuration to the excited state of appropriate symmetry makes the ground state unstable with respect to low-symmetry displacements if the condition of instability (6) is satisfied. The similarity in the substituents R (all of them from the second row except H) allows one to assume (based on previous experience[17,18]) that the energy gap is the main factor in the comparison of the possible instability of these four compounds.

The possible distortions of the high-symmetry configuration of these compounds, similar to the considered above Si_4F_4 case, in the two-level approximation is controlled by the PJTE problems $(1^1B_{2g} + 1^1A_{1u}) \otimes b_{2u}$, $(1^1A_{1g} + 1^1B_{1g}) \otimes b_{1g}$, and $(1^1A_g + 1^1B_{2g}) \otimes b_{2g}$ with energy gaps between the interacting electronic states Δ_1, Δ_2, and Δ_3, respectively. The calculated values of the latter are given in Table 2 (Δ_3 were calculated at the geometry of $Qb_{1g} = 0.74$Å). By comparing the Δ_1 values, we see that they are very close, which indicates that the four molecules have almost equal possibility to form boat-like structures (which, however, are not necessarily ground state structures, see below). The situation is different with the Δ_2 and Δ_3 values. The Δ_2 (0.70 eV) value in Si_4H_4 is approximately twice of those for Si_4F_4 (0.37 eV) and $Si_4(OH)_4$ (0.33 eV). It means that the PJT vibronic coupling along the b_{1g} and hence the possibility of generating a chair-like structure is much lower in Si_4H_4 as compared with the other three molecules. Furthermore, the smaller values of Δ_2 and Δ_3 compared with Δ_1 in the Si_4F_4, Si_4Cl_4 and $Si_4(OH)_4$ molecules lead to a stronger PJTE coupling with b_{1g} and b_{2g} distortions than with b_{2u}, explaining why the chair-like structures in these compounds are more stable than the boat-like ones. In this way the PJTE explains the origin of the main structural features of these Si_4R_4 compounds (R = H, F, Cl, OH), their similarities and differences, by comparing energy gaps to the active excited electronic states.

Similar correlations can be found between the structural features of Si_4R_4 compounds with larger substituents R and their electronic structure by comparing the energy gaps between PJT coupled molecular orbitals instead of electronic states. As shown above, in the D_{4h} configuration the electronic transition from the e_g (HOMO) to the e_u orbitals produces the $^1A_{1u}$ excited electronic state which couples with $^1B_{2g}$ ground state to form the boat-like
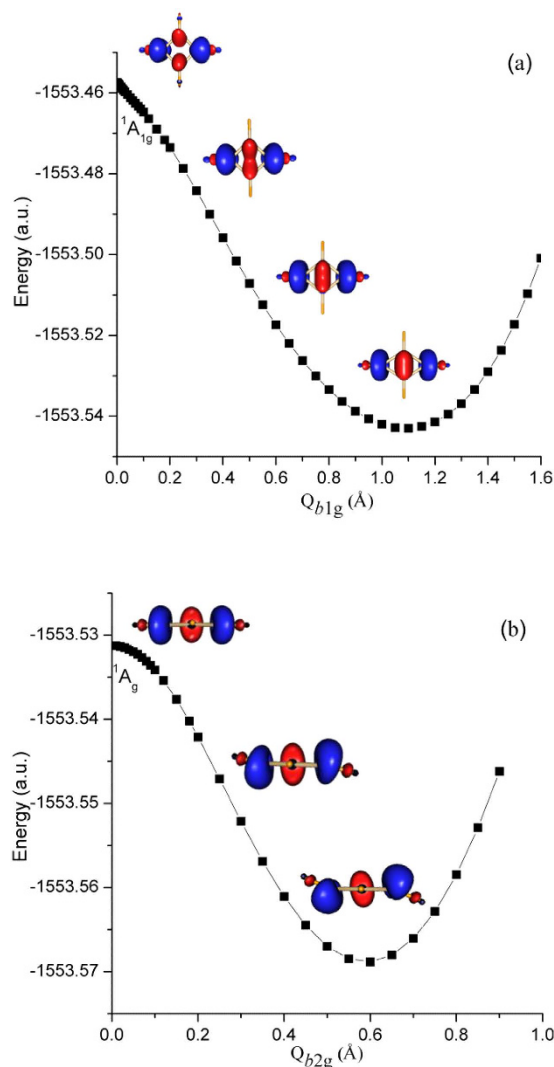
Figure 6. Tracing the HOMO of the Si_4F_4 molecule in the ^1A_g ground state along first b_{1g} (**a**) and second b_{2g} (**b**) distortions. The HOMO actually originates from the empty b_{1g} orbital of the undistorted D_{4h} configuration. The graphic pictures in (**a,b**) are displayed in mutually perpendicular planes.

Structure	PJTE	Energy gap	Si_4H_4	Si_4F_4	Si_4Cl_4	$Si_4(OH)_4$
Boat-like	$\left(1^1B_{2g} + 1^1A_{1u}\right) \otimes b_{2u}$	Δ_1	4.02	3.94	4.19	3.81
		δ_1	4.10	4.91	4.19	4.18
Chair-like	$\left(1^1A_{1g} + 1^1B_{1g}\right) \otimes b_{1g}$ $\left(1^1A_g + 1^1B_{2g}\right) \otimes b_{2g}$	Δ_2	0.70	0.37	0.51	0.33
		Δ_3	1.41	1.50	1.02	1.30
		δ_2	3.98	1.47	1.86	1.34
		δ_3	3.71	1.38	1.51	1.23

Table 2. Energy gaps (in eV) between PJT interacting electronic states Δ_1, Δ_2, and Δ_3, and PJT coupled molecular orbitals δ_1, δ_2, and δ_3, in the PJTE formulations of the boat-like and chair-like structures of Si_4H_4, Si_4F_4, Si_4Cl_4, and $Si_4(OH)_4$ molecules.

structure, while the electronic transition from e_g to the empty a_{1g} or b_{1g} orbitals plays a key role in the formation of the chair-like structure. The calculated energy gaps of the e_u, a_{1g} and b_{1g} empty orbitals relative to the e_g (HOMO) orbitals in the D_{4h} configuration denoted by δ_1, δ_2, and δ_3, respectively, are given in Table 2. It is seen that the δ_1 for all the four molecules are very close, but the δ_2, δ_3 values for Si_4H_4 are much larger than others, which also confirms that the chair-like structures are preferred in Si_4F_4, Si_4Cl_4 and $Si_4(OH)_4$, but not in Si_4H_4. In addition, the larger values of δ_2, δ_3 than δ_1 in Si_4R_4 (R = F, Cl, OH) lead to the same conclusion as above that the chair-like structures are lower in energy than the boat-like structures.

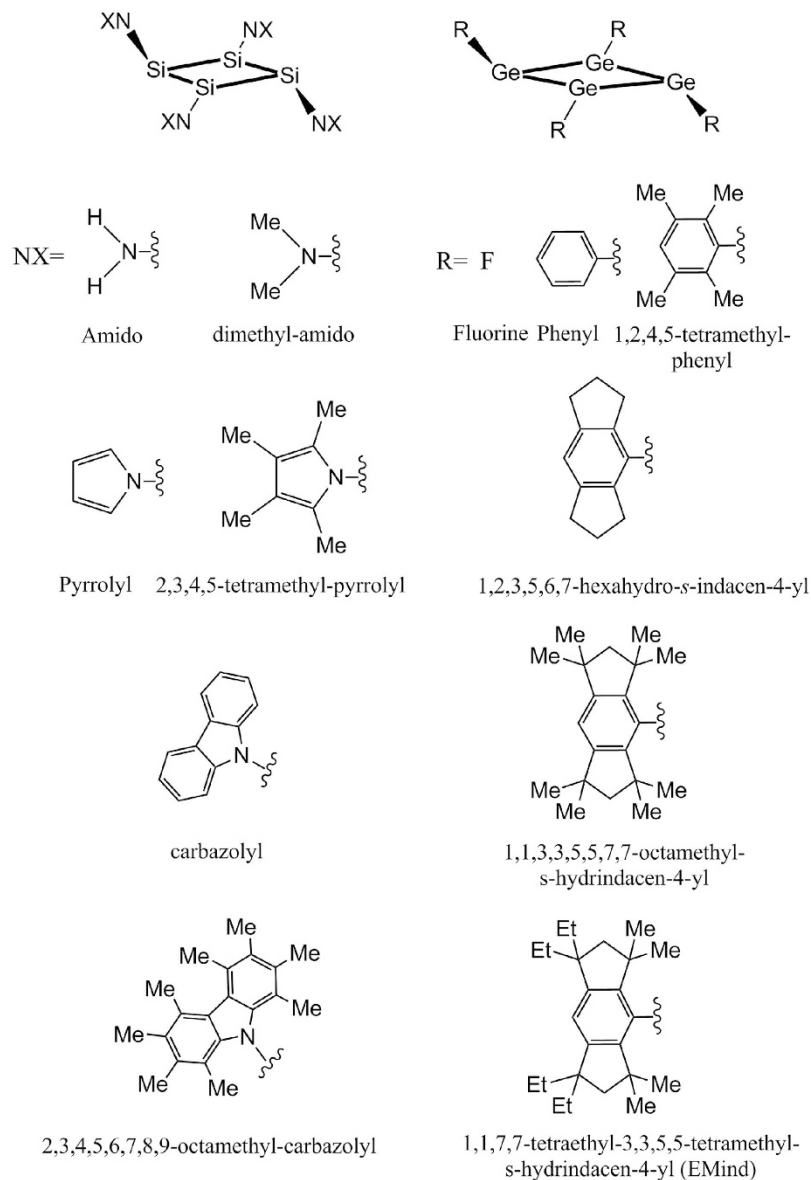**Figure 7. The stable chair-like structures of $Si_4(NX)_4$ and Ge_4R_4 compounds.**

Other analogues: $Si_4(NX)_4$ and Ge_4R_4.

Below in this section we extend the results obtained above for tetrasilacyclobutadiene analogues Si_4R_4 with a characteristic series of substituents R (shown in Fig. 5) to include two other series, namely, $Si_4(NX)_4$ with amido substituents, and Ge_4R_4 which replaces silicon with the heavier germanium element. In the first of these two series, all the $Si_4(NX)_4$ analogues with substituents from NH_2 to larger carbazolyl groups could stabilize in the chair-like structures shown in Fig. 7. Electronic structure calculations with geometry optimization starting with the puckered geometry converge either to the boat-like minimum with higher energy or back to the minimum with the chair-like structures. The latter is thus preferable in all tetrasilacyclobutadiene compounds except Si_4H_4. From the point view of stereoselectivity, the chair-like structure is also preferred because it lowers the steric hindrance induced by large substituents.

As shown above, in the series Si_4R_4 with R as fluorine, phenyl, tetramethyl-phenyl, s-indacene, and the EMind group, the origin of their chair-like structures are due to the PJTE. If the central Si_4 ring is substituted by the Ge_4, the chair-like structures are predicted to be stable too, as shown in Fig. 7. Calculated structural and electronic parameters for the Ge_4R_4 and Si_4R_4 series with the same substituents R are given in Table 3. The four-member ring in Ge_4R_4 and Si_4R_4 is planar and rhombic: the dihedral angle is very close to 0°, and the sum of the internal bond angles is very close to 360°, the bond length of the four Ge-Ge or Si-Si bonds are also very similar. As expected, the bond distances of the Ge-Ge bonds are longer than those of Si-Si bonds due to the bigger atomic radius of germanium than that of the silicon atom. Moreover, we found that the HOMO-LUMO gaps in the equilibrium configuration of most of Ge_4R_4 compounds are larger than those of Si_4R_4, especially in $Ge_4(EMind)_4$. The larger HOMO-LUMO gap *ceteris paribus* means the bigger hardness and higher stability with respect to external perturbations. Therefore, the Ge_4R_4 compounds with relatively large size substituents are predicted to have a stronger

R	Si$_4$R$_4$		Ge$_4$R$_4$	
	ΔE	d$_{Si-Si}$	ΔE	d$_{Ge-Ge}$
Fluorine	3.74	2.309/2.309/2.309/2.309	3.21	2.458/2.458/2.458/2.458/
Phenyl	2.39	2.298/2.298/2.298/2.298	2.79	2.373/2.373/2.392/2.392
1,2,4,5-tetramethyl -phenyl	2.39	2.298/2.298/2.310/2.310	2.34	2.374/2.374/2.374/2.374/
1,2,3,5,6,7-hexahydro -s-indacen-4-yl	2.18	2.298/2.298/2.301/2.301	2.66	2.367/2.367/2.397/2.397/
1,1,3,3,5,5,7,7 -octamethyl- -s-hydrindacen-4-yl	1.87	2.313/2.313/2.328/2.328	2.02	2.369/2.369/2.376/2.376
EMind	1.86	2.311/2.315/2.323/2.331	2.11	2.370/2.371/2.376/2.379

Table 3. The HOMO-LUMO energy gaps ΔE (in eV) and bond distances d$_{Si-Si}$, d$_{Ge-Ge}$ (in Å) for the chair-like structures of Si$_4$R$_4$ and Ge$_4$R$_4$ compounds with different substituents R.

tendency to stabilize in the chair-like structures than the corresponding Si$_4$R$_4$ analogues. These predictions for Si$_4$(NX)$_4$ and Ge$_4$R$_4$ analogues may be useful in the search of potential precursors for semiconducting materials.

Computational Methods. The geometry optimization and frequency calculations for the equilibrium structures of Si$_4$R$_4$ or Ge$_4$R$_4$ analogues are performed by the density functional theory with the B3LYP functional[34,35] of the Gaussian 03 program[36]. Electronic excited states and potential energy profiles along different vibrational modes are obtained by the complete active space self-consistent field (CASSCF) method[37,38] as implemented in MOLPRO 2010 packages[39] based on the optimized geometries and normal coordinates of the ground state ($^3A_{2g}$) at the square configuration of D$_{4h}$ symmetry by B3LYP method. The adiabatic potential energy surface in the lowest electronic state is obtained with B3LYP. The active space in the CASSCF method is composed of six electrons and all the valence empty orbitals, i.e., CAS(6,13) for Si$_4$H$_4$, Si$_4$F$_4$, and Si$_4$Cl$_4$, and CAS(6,17) for Si$_4$(OH)$_4$. The 6-31g(d,p) basis set is employed for all the calculations in this study.

Conclusions

The PJTE is shown to be instrumental in revealing the main structural features of a series of tetrasilacyclobutadiene analogues, Si$_4$R$_4$ and Ge$_4$R$_4$, including large-size substituents, and rationalizing their similarities and differences. In all these compounds the excited electronic states that induce the deformation of the high-symmetry configuration in the ground state are determined, providing for a tool of possible manipulation of the structure (restoration of the planar configuration) by means of external perturbations. The formation of the boat-like structures originates from the PJTE vibronic coupling problem $(1^1B_{2g} + 1^1A_{1u}) \otimes b_{2u}$ in the D$_{4h}$ configuration, and the formation of chair-like structures is due to the PJT interaction of $(1^1A_{1g} + 1^1B_{1g} + 2^1A_{1g}) \otimes b_{1g}$ followed by the $(1^1A_g + 1^1B_{2g} + 2^1A_g) \otimes b_{2g}$. The qualitative analysis of the PJTE is enhanced by numerical estimates of the main vibronic coupling constants. Taking Si$_4$H$_4$, Si$_4$F$_4$, Si$_4$Cl$_4$ and Si$_4$(OH)$_4$ as examples, the substituent effect is analyzed, their structural differences shown to be due to the differences in the energy gaps to the PJT active excited states or between corresponding molecular orbitals. For Si$_4$R$_4$ with large substituents the same PJTE origin of preferred chair-like structures is deduced from their frontier molecular orbitals. For the Si$_4$(NX)$_4$ analogues with amido substituents and Ge$_4$R$_4$ homologs, the chair-like structures are still prefered. By comparison of the bonding character and HOMO-LUMO gaps in Ge$_4$R$_4$ and Si$_4$R$_4$ it is shown that the Ge$_4$R$_4$ compounds are expected to be more stable in the chair-like structures than the corresponding Si$_4$R$_4$ analogues, especially with the large-size substituents.

References

1. Yates, B. F., Clabo Jr, D. A. & Schaefer, III, H. F. Cyclic isomers of singlet Si$_4$H$_4$ related to tetrasilacyclobutadiene. *Chem. Phys. Lett.* **143,** 421–427 (1988).
2. Gunion, R. F., Koppel, H., Leach, G. W. & Lineberger, W. C. Photoelectron spectroscopy of C$_4$H$_4^-$: Ab initio calculations and dynamics of the 1,2-hydrogen shift in vinylvinylidene. *J. Chem. Phys.* **103,** 1250–1262 (1995).
3. Shiota, Y., Kondo, M. & Yoshizawa, K. Role of molecular distortions in the spin-orbit coupling between the singlet and triplet states of the 4π electron systems C$_4$H$_4$, C$_5$H$_5^+$, and C$_3$H$_3^-$. *J. Chem. Phys.* **115,** 9243–9254 (2001).
4. Legrand, Y.-M., van der Lee, A. & Barboiu, M. Single-Crystal X-ray Structure of 1,3-Dimethylcyclobutadiene by Confinement in a Crystalline Matrix. *Science* **329,** 299–302 (2010).
5. Nazari, F. & Doroodi, Z. The substitution effect on heavy versions of cyclobutadiene. *Int. J. Quantum Chem.* **110,** 1514–1528 (2010).
6. Wu, J. I., Evangelista, F. A. & Schleyer, P. v. R. Why Are Perfluorocyclobutadiene and Some Other (CF)$_n^q$ Rings Non-Planar? *Org. Lett.* **12,** 768–771 (2010).
7. Liu, Y., Bersuker, I. B., Garcia-Fernandez, P. & Boggs, J. E. Pseudo Jahn–Teller Origin of Nonplanarity and Rectangular-Ring Structure of Tetrafluorocyclobutadiene. *J. Phys. Chem. A* **116,** 7564–7570 (2012).
8. Wu, J. I. C., Mo, Y. R., Evangelista, F. A. & Schleyer, P. V. Is cyclobutadiene really highly destabilized by antiaromaticity? *Chem. Commun.* **48,** 8437–8439 (2012).
9. Mullinax, J. W., Hollman, D. S. & Schaefer, H. F. Tetragermacyclobutadiene: energetically disfavored with respect to its structural isomers. *Chem. Eur. J* **19,** 7487–7495 (2013).
10. Kickelbick, G. The diverse world of silicon chemistry. *Angew. Chem. Int. Edit.* **44,** 6804–6806 (2005).
11. Suzuki, K. *et al.* A planar rhombic charge-separated tetrasilacyclobutadiene. *Science* **331,** 1306–1309 (2011).
12. Apeloig, Y. The diamond within a silicon analog of cyclobutadiene. *Science* **331,** 1277–1278 (2011).
13. Inoue, S., Epping, J. D., Irran, E. & Driess, M. Formation of a donor-stabilized tetrasilacyclobutadiene dication by a lewis acid assisted reaction of an N-heterocyclic chloro silylene. *J. Am. Chem. Soc.* **133,** 8514–8517 (2011).
14. Zhang, S.-H., Xi, H.-W., Lim, K. H. & So, C.-W. An extensive n, π, σ-electron delocalized Si$_4$ Ring. *Angew. Chem. Int. Edit.* **52,** 12364–12367 (2013).
15. Lee, V. Y., Ito, Y., Yasuda, H., Takanashi, K. & Sekiguchi, A. From tetragermacyclobutene to tetragermacyclobutadiene dianion to tetragermacyclobutadiene transition metal complexes. *J. Am. Chem. Soc.* **133,** 5103–5108 (2011).

16. Yeong, H. X. *et al.* An amidinate-stabilized germatrisilacyclobutadiene ylide. *Chem. Eur. J.* **18,** 2685–2691 (2012).
17. Bersuker, I. B. *The Jahn-Teller Effect* (Cambridge University Press, Cambridge, UK (2006).
18. Bersuker, I. B. Pseudo-Jahn–Teller effect—a two-state paradigm in formation, deformation, and transformation of molecular systems and solids. *Chem. Rev.* **113,** 1351–1390 (2013).
19. Bersuker, I. B. In *Advances in Chemical Physics* Vol. 160 (eds Rice, S. & Dinner, R.) Ch. 3, In press (Wiley, 2016).
20. Koseki, S. & Toyota, A. Energy component analysis of the Pseudo-Jahn−Teller effect in the ground and electronically excited states of the cyclic conjugated hydrocarbons: cyclobutadiene, benzene, and cyclooctatetraene. *J. Phys. Chem. A* **101,** 5712–5718 (1997).
21. Garcia-Fernandez, P., Bersuker, I. B. & Boggs, J. E. Pseudo-Jahn-Teller origin of geometry and pseudorotations in second row tetra-atomic clusters X_4 (X = Na, Mg, Al, Si, P, S). *J. Chem. Phys.* **124,** 044321 (2006).
22. Liu, Y., Bersuker, I. B. & Boggs, J. E. Pseudo Jahn–Teller origin of puckering in $C_4H_4^{2+}$, $Si_4H_4^{2+}$ and $C_4F_4^{2+}$ and dications. *Chem. Phys.* **417,** 26–29 (2013).
23. Liu, Y., Bersuker, I. B., Zou, W. & Boggs, J. E. Pseudo Jahn-Teller versus Renner-Teller effects in the instability of linear molecules. *Chem. Phys.* **376,** 30–35 (2010).
24. Kayi, H., Bersuker, I. B. & Boggs, J. E. Pseudo Jahn–Teller origin of bending instability of triatomic molecules. *J. Mol. Struct.* **1023,** 108–114 (2012).
25. Ilkhani, A. R., Gorinchoy, N. N. & Bersuker, I. B. Pseudo Jahn–Teller effect in distortion and restoration of planar configurations of tetra-heterocyclic 1,2-diazetes $C_2N_2E_4$, E = H, F, Cl, Br. *Chem. Phys.* **460,** 106–110 (2015).
26. Bhattacharyya, S., Opalka, D. & Domcke, W. Jahn–Teller effect in the cation and its signatures in the photoelectron spectrum of P_4. *Chem. Phys.* **460,** 51–55 (2015).
27. Boltrushko, V., Krasnenko, V. & Hizhnyakov, V. Pseudo Jahn–Teller effect in stacked benzene molecules. *Chem. Phys.* **460,** 90–96 (2015).
28. Soto, J. R., Molina, B. & Castro, J. J. Reexamination of the origin of the pseudo Jahn-Teller puckering instability in silicene. *Phys. Chem. Chem. Phys.* **17,** 7624–7628 (2015).
29. Bersuker, I. B. In *Jahn-Teller Effect: Fundamentals and Implications for Physics and Chemistry* Vol. 97 (eds Koppel, H., Yarkony, D. R. & Barentzen, H.) Ch. 1, 3–23. (Springer-Verlag Berlin, Berlin, 2009).
30. Jose, D. & Datta, A. Structures and Chemical Properties of Silicene: Unlike Graphene. *Acc. Chem. Res.* **47,** 593–602 (2014).
31. Ivanov, A. S., Bozhenko, K. V. & Boldyrev, A. I. On the suppression mechanism of the Pseudo-Jahn–Teller effect in middle E_6 (E = P, As, Sb) rings of triple-decker sandwich complexes. *Inorg. Chem.* **51,** 8868–8872 (2012).
32. Pokhodnya, K. *et al.* Flattening a puckered cyclohexasilane ring by suppression of the pseudo-Jahn–Teller effect. *J. Chem. Phys.* **134,** 014105 (2011).
33. Hermoso, W., Ilkhani, A. R. & Bersuker, I. B. Pseudo Jahn–Teller origin of instability of planar configurations of hexa-heterocycles $C_4N_2H_4X_2$ (X = H, F, Cl, Br). *Comput. Theor. Chem.* **1049,** 109–114 (2014).
34. Becke, A. D. Density-functional exchange-energy approximation with correct asymptotic behavior. *Phys. Rev. A* **38,** 3098–3100 (1988).
35. Lee, C., Yang, W. & Parr, R. G. Development of the colle-salvetti correlation-energy formula into a functional of the electron density. *Phys. Rev. B* **37,** 785–789 (1988).
36. Frisch, M. J. *et al.* Gaussian 03, Revision E.01. Gaussian, Inc (2004).
37. Knowles, P. J. & Werner, H.-J. An efficient second-order MCSCF method for long configuration expansions. *Chem. Phys. Lett.* **115,** 259–267 (1985).
38. Werner, H.-J. & Knowles, P. J. A second order multiconfiguration SCF procedure with optimum convergence. *J. Chem. Phys.* **82,** 5053–5063 (1985).
39. Werner, H.-J. *et al.* MOLPRO, version 2010.1 (2010).

Acknowledgements

Author Contributions

Y.L. and I.B. designed the research and wrote the main manuscript text; Y.L. and Y.W. performed the calculations and prepared the figures. All authors reviewed the manuscript.

Additional Information

Supplementary information accompanies this paper at http://www.nature.com/srep

Competing financial interests: The authors declare no competing financial interests.

How to cite this article: Liu, Y. *et al.* Geometry, Electronic Structure, and Pseudo Jahn-Teller Effect in Tetrasilacyclobutadiene Analogues. *Sci. Rep.* **6,** 23315; doi: 10.1038/srep23315 (2016).